Lasers in Manufacturing Conference 2017

Resistance modification of diamond through silicon incorporation

Markus Prieske[a,*], Frank Vollertsen[a,b]

[a]*BIAS – Bremer Institut für angewandte Strahltechnik GmbH, Klagenfurter Str. 5, 28359 Bremen, Germany*
[b]*University of Bremen, Bibliothekstr. 1, 28359 Bremen, Germany*

Abstract

The application of polycrystalline diamond coatings in the industrial sector is rising due to its outstanding properties. They are for example deployed for heat sinks in electrical circuits because of the high thermal conductivity. Diamond is an electrical insulator with a resistance higher than 10^{10} Ω. For applications as in semiconductor technologies or to avoid static electricity in components induced by friction, diamond coatings with a lower electrical resistance are necessary. The aim of this study was to modify the resistance of diamond coatings through silicon incorporation. The polycrystalline diamond coatings were deposited by a laser-based plasma chemical vapour deposition (CVD) process without a chamber at atmospheric pressure. The in situ silicon incorporation was realised by the supply of a solid silicon carbide precursor into the plasma flame during the CVD process. The evaporation of silicon during diamond growth induced impurities into the diamond layer. The crystal structure of the diamond films was verified by Raman spectroscopy and scanning electron microscopy (SEM). To analyse the distribution of the incorporated silicon, focused ion beam profiles were produced and recorded by scanning electron microscopy. Hereby it was shown that the silicon is incorporated underneath as well as in between the polycrystalline diamonds. Furthermore, a doping of the diamond crystals was archived which is proved by a sharp peak at 738 nm in the luminescence spectra. That peak is characteristic for the existence of silicon-vacancy centres. Using backscattered electron microscopy (BSE), it was detected that the silicon content in the centre of the process position is lower than at the edges. This led to a variation of the resistance from kΩ at the edges to higher than 60 MΩ in the centre of the coating. A sheet resistance of 2.43 MΩ ± 1.98 MΩ was measured by a 4-point probe van der Pauw resistivity measurement on a single diamond crystal in the centre of the coating.

Keywords: polycrystalline CVD-diamond; coatings; resistance modification;

* Corresponding author. Tel.: +49-421-21858113; fax: +49-421-21858063.
E-mail address: prieske@bias.de

1. Introduction

The application of polycrystalline diamond coatings in the industrial sector is rising due to its outstanding properties. They are for example deployed for heat sinks in electrical circuits because of the high thermal conductivity. Diamond is an electrical insulator with a resistance higher than $10^{10}\ \Omega$, Tsigkourakos et al., 2014. For applications as in semiconductor technologies or to avoid static electricity in components induced by friction, diamond coatings with a lower electrical resistance are necessary. Boron is the impurity that is most widely used to manipulate the electrical conductivity to achieve p-type doping of diamond, Kraft, 2007. Tsigkourakos et al., 2014 achieved a resistance of $10^{6}\ \Omega$ by boron doping. To introduce n-type doping, nitrogen (N), phosphorus (P), or arsenic (As) is used, Kalish, 1999. In this study we investigate to incorporate silicon impurities into a diamond coating to analyze the influence onto the resistance. If silicon incorporates into diamond crystals, so called silicon-vacancy (SiV) centers are formed, which have a sharp zero phonon line at 738 nm with only weak vibrational sidebands at room temperature, Sternschulte et al., 1994. This can be used to proof the successful silicon doping of diamond. In literature different ways of incorporation of silicon into diamond coatings are reported. Rogers et al., 2014 used microwave plasma chemical vapour deposition (CVD) to create in situ single bright SiV centres in high quality, low stress single-crystalline CVD-diamond. By using a high microwave input power for the deposition process, silicon was etched off the quartz glass windows of the vacuum chamber by the plasma. Teraji et al., 2015, used a silicon carbide plate placed underneath the substrate to induce SiV centres. In this way, SiV concentrations in the ppb range could be incorporated. Wang et al., 2006, produced SiV centres in diamond via ion implantation and Sedov et al., 2015 mixed silane gas with the process gases.

2. Methods

A CO_2 laser-based plasma CVD process was used at atmospheric pressure without a vacuum chamber for the deposition of polycrystalline CVD-diamond coatings. The CVD process is combined with an in situ physical vapour deposition (PVD) process by introducing solid silicon carbide precursors into the plasma flame, which is described in detail by Schwander et al., 2014. The combined PVD process is used to introduce the impurities into the CVD-diamond layer. The research facility setup of the laser-based plasma CVD process is shown in Fig. 1.

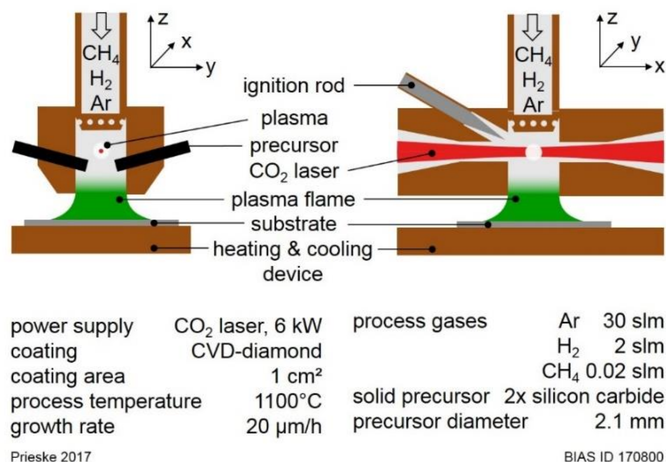

Fig. 1. Schematic layout of the laser induced plasma CVD process at atmospheric pressure.

A 6 kW high-power CO_2 laser with a wavelength of 10.6 µm is used for energy supply of the argon plasma jet. The ignition of the plasma flame is achieved by thermionic emission through inserting a tungsten lanthanum electrode into the laser focus. This generates an optical breakdown. After the ignition of the argon plasma flame, the process gases methane (0.02 standard litres per minute (slm)) and hydrogen (2.3 slm), which are required for CVD synthesis of polycrystalline diamond, are introduced.

Two solid silicon carbide bars (high-tech ceram®-SSiC) with a squared cross-section and a side length of 2.1 mm are used as precursors for the in situ PVD process. The purity of the silicon carbide bars is higher than 99 %. The precursors are inserted by feed units using DC-servomotors with a positional accuracy of 0.1 mm. The amount of sublimated silicon carbide was kept constant during CVD-diamond deposition by keeping the intensity of the silicon peak of the measured emission spectra constant through feeding the precursor into the plasma flame. To adjust the amount of evaporated silicon carbide for different samples, a certain ratio between the silicon (Si) and carbide (C2) peaks, which are marked by blue lines in Fig. 2, was determined. The methane gas in the used gas composition has the main impact on the intensity of the C2-peak. The weights of the two precursors were determined before and after the coating deposition with an accuracy of 1 mg. The evaporation rate was calculated from the quotient of the amount of silicon carbide evaporated and the duration of deposition. A Keyence VHX-1000 microscope was used to determine the surface area of the CVD-diamond coating with incorporated silicon.

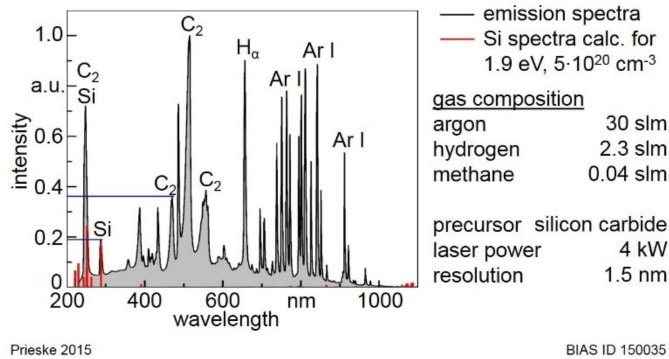

Fig. 2. Emission spectra of the plasma flame (Ar, H_2, CH_4) with inserted silicon carbide bars, with calculated silica spectra (electron temperature 1.9 eV and electron density $5 \cdot 10^{20}$ cm^{-3}, NIST, 2016).

As substrates molybdenum sheets were used with a grinded surface by a silicon carbide grinding paper (grit 320). The diamond nucleation was carried out with a dispersion consisting of 200 ml of isopropanol and 210 mg of diamond powder with an average crystal size of 0.25 µm to 0.50 µm from the company Microdiamant AG. The substrates were put into the dispersion for ten minutes in an ultrasonic bath and subsequently into isopropanol for three minutes. The CVD-diamond coating with incorporated silicon was deposited for 40 minutes. The temperature measured by thermocouples from underneath the substrate was regulated at 880 °C during deposition by feedback control. Detailed implementation of the feedback control was published by Prieske et al., 2015. This regulated temperature results in a surface temperature of 1050 °C measured by IMPAC pyrometer IGAR 12-LO.

To determine the influence on the resistivity, 2-point resistance measurements were executed using a Fluke 117 multimeter with a measuring tip distance of 2 mm. At the Fraunhofer ISC in Würzburg four-point probe van der Pauw resistivity measurements have been executed. Four contacts have been arranged on a single diamond crystal. A current *I* has been applied at two neighbouring contacts and the voltage was

measured at the other two contacts. The contacts have been cyclically exchanged. The sheet resistance ρ was then calculated using the van der Pauw method, van der Pauw, 1958.

3. Results

In Fig. 3 the polycrystalline structure of the CVD-diamond coating can be seen in the scanning electron (SE) microscope images. Even though silicon carbide rods were evaporated during diamond deposition, the quality of the diamond crystals evaluated according to the sharpness of the crystal edges remains. The backscattering electron (BSE) microscope image at the bottom left of Fig. 3 show white particles on top of the diamond crystals at the border of the coated area. These particles are proved to be silicon by wavelength-dispersive X-ray spectroscopy (WDX). At the centre of the coating no white particles could be detected in the BSE image. A WDX measurement on a diamond crystal did not show any silicon signal at all, which shows that the incorporated silicon content in the diamond crystals is lower than the detection limit of the used WDX system. The CVD-coating was proved to be diamond by measuring a distinct peak at 1337 cm^{-1} by Raman spectroscopy (see Fig. 4a) and by the visible polycrystalline structure according to the SE images (see Fig. 3), Ferrari and Robertson, 2000. More detailed information of the intensity of the diamond peak in Raman spectroscopy over the whole coating are published by Prieske and Vollertsen, 2016.

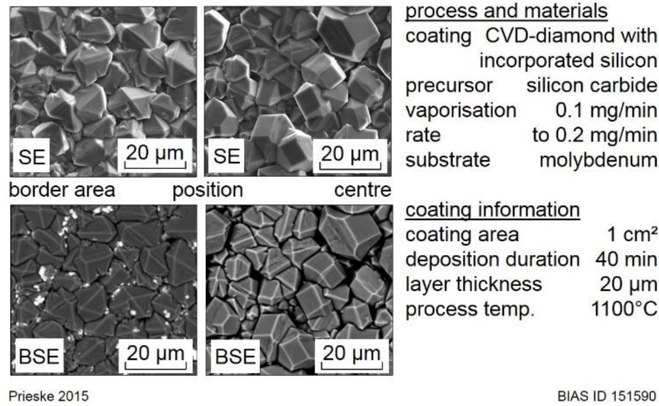

Fig. 3. Scanning electron (SE) and backscattering electron (BSE) microscope image of the CVD-diamond coating at the border area and centre of the coating area.

A distinct peak can be detected in the Raman spectra at a Raman shift of 1337 cm^{-1} in Fig. 4a. Compared to the residual stress free diamond peak at 1332 cm^{-1} Ferrari and Robertson, 2000, the diamond peak shifted about $\Delta\omega_0 = 5$ cm^{-1}. The present residual compressive stress can be calculated with the formula,

$$\sigma = -A \times \Delta\omega_0 \quad (1)$$

using the empirical constant A = 0.345 GPa/cm^{-1} investigated at polycrystalline diamond coatings by Ferreira et al., 2003. This results in a residual compressive stress of 1.7 GPa.

The photoluminescence spectrum of a single diamond crystal of the diamond coating with incorporated silicon shows a distinct peak at 738 nm with a full width at half maximum of 7 nm (see Fig. 4b), which is the position at which Sternschulte et al., 1994 located the emission wavelength of single photon emission from SiV centres in diamond. This proves that the diamond coating is doped by a small silicon content without having an impact on the diamond structure.

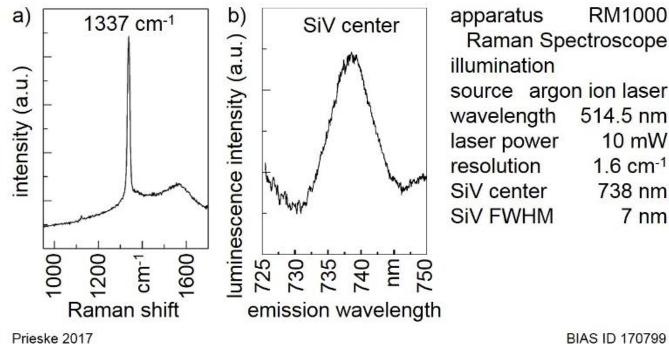

Fig. 4. (a) Raman spectrum and (b) photoluminescence spectrum of the diamond coating with incorporated silicon.

Fig. 5 shows that the CVD-diamond coating area decreases with increasing evaporation rate of the silicon carbide precursors. With an evaporation rate of 0.22 mg/min, the surface area of the diamond layer decreases to approximately 25 mm^2. In contrast, an evaporation rate below 0.025 mg/min leads to a CVD-diamond surface area of 140 mm^2.

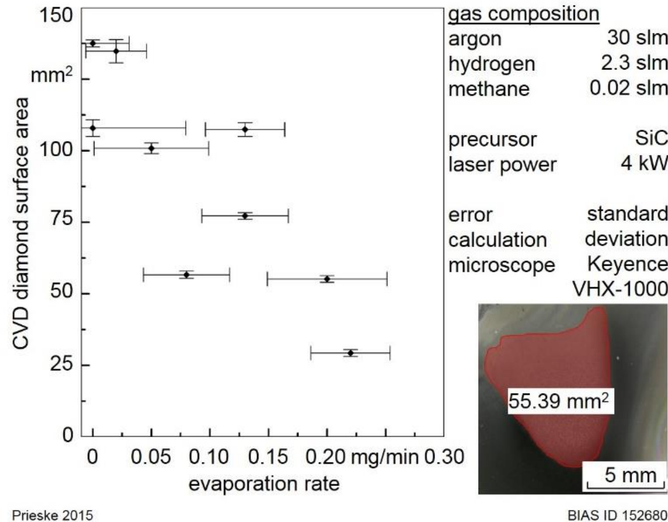

Fig. 5. Surface area of the CVD-diamond coating as a function of the evaporation rate of silicon carbide.

Focused ion beam (FIB) profiles where executed at the border area of the coating, shown in Fig. 6, which give further insight into the silicon distribution. In Fig. 6a a silicon cluster that reaches into an adjoining diamond crystal can be seen. Fig. 6b shows silicon in the form of an intermediate layer between the molybdenum substrate and the diamond crystal. Furthermore, Figs. 6c and 6d show that silicon clusters that are integrated into diamond crystals also exist.

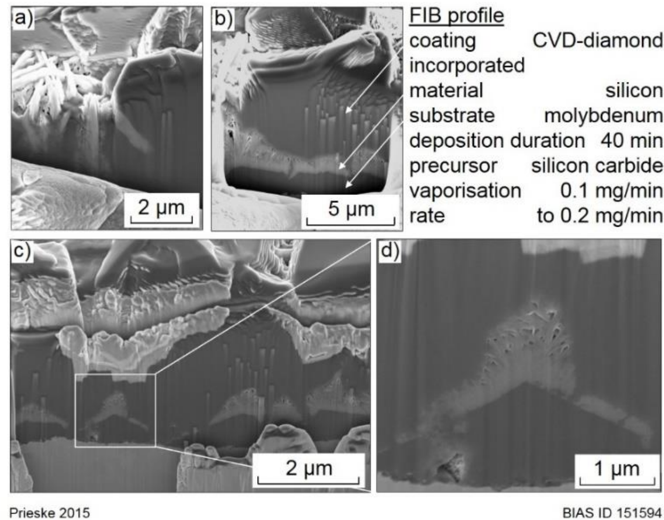

Fig. 6. Focused ion beam (FIB) profile showing that the incorporated silicon (bright grey) is located: (a) extending into, (b) underneath, (c) and (d) integrated into the CVD-diamond crystals.

2-point resistance measurements were executed and the resistance results were merged to a resistance map (Fig. 7 top left). At the border area of the diamond coating resistances in the Ohm range could be measured. Approaching the centre of the diamond coating the resistance increased until the upper measuring limit of 60 MΩ was reached, so that the resistance could not be measured with the used multimeter. On a CVD-diamond coating without incorporated silicon the resistance is higher than the upper measuring limit of 60 MΩ all over the coating.

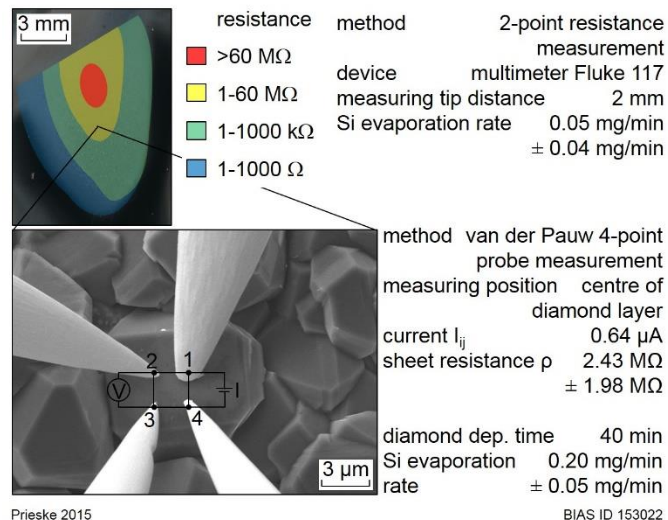

Fig. 7. Resistance map measured by 2-point resistance and resistivity measurement by 4-point probe van der Pauw method on a single diamond crystal (measurement done at Fraunhofer ISC, Würzburg).

A 4-point probe van der Pauw resistivity measurement was carried out on a single diamond crystal, which is shown in Fig. 7 bottom. The diamond crystal was located in the centre of the deposited CVD-diamond coating. A sheet resistance ρ of 2.43 MΩ ± 1.98 MΩ was measured.

4. Discussion

In FIB profiles, it is shown that the polycrystalline diamond layer is actually penetrated by a silicon network. Therefore the determination of the critical silicon content inside a diamond crystal is challenging, because the content that is incorporated in a single diamond crystal lattice is too low to be detectable by WDS measurement. A discrete value for the silicon content in the coating cannot be given according to the inhomogeneous distribution of silicon. Therefore, the critical evaporation rate instead of the critical silicon content was experimentally determined until no diamond layer was grown. The surface area of the CVD-diamond coating as a function of the evaporation rate of silicon carbide shows that an evaporation rate higher than 0.22 mg/min leads to a CVD diamond surface area smaller than 25 mm^2. The graph in Fig. 5 implies that CVD diamond growth stops if the evaporation rate exceeds 0.3 mg/min. It could also be seen that the in situ evaporation of silicon carbide decelerates the growth rate of the CVD-diamond coating. The lateral silicon carbide precursor supply into the plasma flame leads to a higher silicon concentration at the outer zone of the plasma flame. With an increasing evaporation rate, the area in the plasma flame where the critical silicon concentration is exceeded grows, from outer zone of the plasma flame towards the inner zone, so that the area where diamond is still growing decreases as can be seen in Fig. 5. On measuring the luminescence spectrum of the diamond layer with incorporated silicon, a peak at 738 nm can be detected, which verifies that doping of the diamond coating by silicon is successfully realized in the executed researches, Sternschulte et al., 1994. This shows that silicon is deposited between the diamond crystals as well as the diamond crystal lattice is doped by silicon atoms.

By 2-point resistance measurements a change in resistance from the Ohm range at the border of the coating up to higher than 60 MΩ at the centre of the coating could be detected. The very low resistance in the Ohm range at the border area could originate from a prevailing high density of silicon cluster (see fig. 5). On a CVD-diamond coating without incorporated silicon the resistance is higher than the upper measuring limit of 60 MΩ all over the coating. According to Tsigkourakos et al., 2014 the resistance of an undoped diamond crystal is higher than 10 GΩ. The application of a 4-point probe van der Pauw resistivity measurement on a single CVD-diamond crystal in the centre of the coating leads to a sheet resistance of 2.43 MΩ ± 1.98 MΩ.

5. Conclusion

From the luminescence and resistivity measurements it can be concluded that adding silicon to the laser induced plasma decreases the electrical resistivity of the coating not only by a silicon deposition between the diamond crystals, but also by a doping of the crystal lattice itself.

Acknowledgements

This work was supported by the Deutsche Forschungsgemeinschaft (DFG) under contract no. VO 530/75-2, which the authors gratefully acknowledge.

References

Ferrari, A.C., Robertson, J., 2000. Interpretation of Raman spectra of disordered and amorphous carbon, Physical Review B 61, pp. 14095–14107

Ferreira, N.G., Abramof, E., Corat, E.J., Trava-Airoldi, V.J., 2003. Residual stresses and crystalline quality of heavily boron-doped diamond films analysed by micro-Raman spectroscopy and X-ray diffraction, Carbon 41, pp. 1301-1308

Guo, Y., Feng, Y., Zhang, L., 2016. Revealing the growth mechanism of SiV centers in chemical vapor deposition of diamond, Diamond and Related Materials 61, pp. 91–96

Kalish, R., 1999. Doping of diamond, Carbon 37 pp. 781–785

Kraft, A., 2007. Doped Diamond: A Compact Review on a New, Versatile Electrode Material, International Journal of Electrochemical Science 2, pp. 355–385

NIST National Institute of Standards and Technology, 2016. Atomic Spectra Database Lines Form http://physics.nist.gov/PhysRefData/ASD/lines_form.html

Prieske, M., Vollertsen, F., 2016. In situ incorporation of silicon into a CVD-diamond layer deposited under atmospheric conditions, Diamond and Related Materials 65, pp. 47-52.

Prieske, M., Wiegmann, C., Schwander, M., Vollertsen, F., 2015. Feedback control of the substrate surface temperature in a laser-induced plasma CVD process, Dry Metal Forming OAJ FMT 1, pp. 1–4

Rogers, L.J., Jahnke, K.D., Metsch, M.H., Sipahigil, A., Binder, J.M., Teraji, T., Sumiya, H., Isoya, J., Lukin, M.D., Hemmer, P., Jelezko, F., 2014. All-optical initialization, readout, and coherent preparation of single silicon-vacancy spins in diamond, Physical Review Letters 113 (26), pp. 263602–263606

Schwander, M., Vollertsen, F., 2014. In situ doping of diamond coatings with silicon, aluminum and titanium through a modified laser-based CVD process, Diamond and Related Materials 41, pp. 41–48

Sedov, V., Ralchenko, V., Khomich, A.A., Vlasov, I., Vul, A., Savin, S., Goryachev, A., Konov,V., 2015. Si-doped nano- and microcrystalline diamond films with controlled bright photoluminescence of silicon-vacancy color centers, Diamond and Related Materials 56, pp. 23–28

Sternschulte, H., Thonke, K., Sauer, R., Munzinger, P.C., Michler, P., 1994. 1.681-eV luminescence center in chemical-vapor-deposited homoepitaxial diamond films, Physical Review B 50, pp. 14554–14560

Teraji, T., Yamamoto, T., Watanabe, K., Koide, Y., Isoya, J., Onoda, S., Ohshima, T., Rogers, L. J., Jelezko, F., Neumann, P., Wrachtrup, J., Koizumi, S., 2015. Homoepitaxial diamond film growth: High purity, high crystalline quality, isotopic enrichment, and single color center formation, Physica status solidi a 212, pp. 2365–2384

Tsigkourakos, M., Hantschel, T., Simon, D.K., Nuytten, T., Verhulst, A.S., Douhard, B., Vandervorst, W., 2014. On the local conductivity of individual diamond seeds and their impact on the interfacial resistance of boron-doped diamond films, Carbon 79, pp. 103-112.

van der Pauw, L. J, 1958. A method of measuring specific resistivity and Hall effect of discs of arbitrary shape, Philips Research Reports 13, pp. 1–9

Wang, C., Kurtsiefer, C., Weinfurter, H., Burchard, B., 2006. Single photon emission from SiV centres in diamond produced by ion implantation, Journal of Physics B: Atomic, Molecular and Optical Physics 39, pp. 37–41